

# Thermoanalytic Studies on Template Removal from MeAPO-31 Doped with Various Metals

Jan Kornatowski,<sup>\*,†,‡</sup> Gerd Finger,<sup>§,||</sup> and Dietrich Schultze<sup>⊥</sup>

*LS II für Technische Chemie, Technische Universität München, D-85747 Garching bei München, Germany, Faculty of Chemistry, Nicholas Copernicus University, PL-87-100 Torun, Poland, Institut für Kristallographie und Mineralogie, Johann-Wolfgang-Goethe-Universität, D-60054 Frankfurt am Main, Germany, and Bundesanstalt für Materialforschung und -prüfung, Labor Thermische Analyse, D-12489 Berlin-Adlershof, Germany*

*Received: June 5, 2001; In Final Form: December 12, 2001*

Removal of the template from MeAPO-31 samples doped with trace amounts of Cu, Cd, Cr, Co, Mn, Mg, and Zn (1 Me heteroatom per 5–115 unit cells) was investigated with thermal analysis methods. The findings were contrasted/compared with mass spectroscopy results. The main factor controlling the material properties is the content of heterocenters and not their chemical identity. The position of the high-temperature differential thermogravimetric peak and the intensity ratio between the high- and low-temperature peaks depend linearly on the content of heteroatoms. Both peaks correspond to thermal degradation and not to a simple release of the template molecules. The low-temperature peak comprises desorption of water to a considerable extent. The linear shift of the position of the high-temperature peak with the metal content reflects a composed phenomenon including a number of (thermo)chemical processes and setting free the species formed during decomposition of the template. This release is significantly hindered by the framework heterocenters. In general, the removal of template is a process controlled by the mobility of the exiting species, and it depends primarily on the content of the heterocenters. The crystal dimensions and the calcination atmosphere also have a significant influence.

## Introduction

Microporous aluminophosphate molecular sieves  $\text{AlPO}_4\text{-}n$ <sup>1</sup> differ from aluminosilicate zeolites with respect to two points: (i) their frameworks, though composed of charged  $\text{AlO}_{4/2}^-$  and  $\text{PO}_{4/2}^+$  tetrahedra, are electrically neutral due to the alternating order of the Al and P units; (ii) they have no ion-exchange properties. Incorporation of additional elements, usually called “heteroatoms”, such as  $\text{Si}^{2+}$  or/and various metals,<sup>3</sup> leads to distinct property changes of substituted MeAP(S)O-*n* materials. As the valence of the introduced elements usually differs from that of an actually substituted element, Al or P, the framework becomes charged. This results in (i) the appearance of ion-exchange properties, (ii) formation of acidic centers in the form of OH groups located at the charged sites of the framework, (iii) modification of catalytic activity, and (iv) changes in sorption/diffusion characteristics.<sup>4</sup>

The hydrothermal synthesis of aluminophosphate molecular sieves usually requires structure-directing agents (templates which are mostly organic amines or their derivatives), which have to be removed from the pores of the crystalline products in a postsynthesis treatment. The commonly applied calcination procedure results in burning off of the organic species and opening the access to the pores for various processes such as sorption, diffusion, etc. Thus, the calcination treatment is one of the most important stages, determining the properties and applicability of the synthesized molecular sieve materials.

Choudhary and Sansare<sup>5</sup> showed the significance of the calcination atmosphere for the removal of template (tripropylamine) from the channels of  $\text{AlPO}_4\text{-}5$ . They presumed this process to be an activated diffusion-controlled desorption in an inert atmosphere and oxidative decomposition under oxygen-deficient conditions because of diffusional limitations in an oxidizing atmosphere. Numerous papers<sup>6–13</sup> have been published on the removal of templates from the pores of various MeAPO-*n* materials substituted with different heteroatoms. However, the investigated materials, e.g., MeAPSO-11,<sup>14</sup> usually contained relatively high amounts of substituted metals. To our knowledge, no work has been devoted to the influence/effect of very low amounts of heteroatoms, although such materials promise an advantage of more perfect or/and complete incorporation of the metals into framework positions. In previous work,<sup>15</sup> we described the synthesis of MeAPO-31 molecular sieves (ATO structure type<sup>16</sup>) containing trace amounts of Zn, Mg, Mn, Co, Cr, Cd, and Cu as dopants in the structure (one Me heteroatom for up to over 100 unit cells (uc's)). The materials were mainly characterized using X-ray diffraction (XRD) methods to determine the influence of the dopants on the structure symmetry of the crystals and their thermal stability.<sup>15</sup>

In the present work, we focus on the thermoanalytic investigations of the doped MeAPO-31 materials and report on the observed effects of the metals, with regard to template removal by calcination. The findings have been verified by a comparison with the results of mass spectroscopy measurements. The ATO system has been chosen for its unidimensional pore system of medium pore size, and a simple template molecule, di-*n*-propylamine, which, in theory, should easily leave the pores with a 0.54 nm diameter.

<sup>†</sup> Technische Universität München.

<sup>‡</sup> Nicholas Copernicus University.

<sup>§</sup> Johann-Wolfgang-Goethe-Universität.

<sup>||</sup> Present address: Märkische Allee 84, D-12681 Berlin, Germany.

<sup>⊥</sup> Labor Thermische Analyse.

## Experimental Section

**Synthesis of Materials.** All the materials were synthesized hydrothermally from reaction mixtures with the following component ratios (as oxides):<sup>15</sup>  $1\text{Al}_2\text{O}_3:1\text{P}_2\text{O}_5:a\text{MeO}$  or  $(a/2)\text{-Cr}_2\text{O}_3:1.7\text{DPA}:280\text{H}_2\text{O}$ , where  $a = 0.005$  or  $0.01$  and DPA is di-*n*-propylamine. The metals Cu, Co, Mn, Mg, Zn, Cd, and Cr taken for substitution (denoted as MeO and  $\text{Cr}_2\text{O}_3$ ) were introduced as sulfates. The reaction gels of  $\text{pH } 3.5 \pm 0.2$  were heated at 463 K in Teflon-lined autoclaves for 48 h. More details are given elsewhere.<sup>15</sup> Prior to the measurements, the samples were dried at 383 K overnight and equilibrated in an air atmosphere of ca. 65% relative humidity for at least 24 h.

**Characterization Methods.** The materials were examined by X-ray diffraction (XRD), temperature-programmed XRD (Guinier technique), light and scanning electron microscopy (SEM), and inductive coupled plasma (ICP) trace analysis (for details and results see ref 15). The mass spectroscopy measurements were carried out with a Thermostat (Balzers) device coupled with a thermobalance SETARAM TAG 24. Thermal gravimetric analyses (TGA) were performed by recording either the differential thermogravimetric (DTG) curves (method 1) or the differential thermogravimetric and thermoanalytic (DTG + DTA) profiles (method 2). The profiles in each figure were normalized to a common sample amount.

**Thermoanalytic Method 1.** The DTG measurements were carried out with a Mettler TA 3000/TG 50 instrument. The samples were heated from 300 to 1273 K at a rate of 10 K/min under oxygen and nitrogen atmospheres introduced at a constant flow rate. Before the experiments, the samples of ca. 15 mg were washed with the stream of the measurement gas for 1 h. The DTG profiles were recorded for the original materials and for the samples ground by hand in an agate mortar.

**Thermoanalytic Method 2.** The DTG and DTA profiles were simultaneously recorded for the samples of ca. 20 mg placed in ceramic beakers and heated from room temperature to 1393 K at a rate of 5 K/min under an air/argon mixture and under pure argon streams (thermobalance SETARAM TAG 24). For the measurements under inert atmosphere, the samples were evacuated before the measurement in situ to  $<1$  mbar, and then the apparatus was filled with argon. This method was applied for the selected ZnAPO-31 and MnAPO-31 materials in the form of the original and ground crystals.

## Results and Discussion

**Materials.** The synthesized phases of ATO type were composed of aggregated prismatic crystals ca.  $50 \mu\text{m}$  long and overgrown along their *c*-axes [001] (Figure 1). The products revealed a narrow distribution of crystal dimensions and could easily be separated from differently sized byproducts. This way, samples of purity higher than 95 wt % were obtained. Despite the identical synthesis conditions and amounts of metal salts used in the reaction gels, the metals were incorporated into the crystals in considerably different amounts.<sup>15</sup> Their content varied from 4.7 (Zn) to 114.5 (Cr) unit cells per metal atom (Table 1). More detailed characteristics have been reported elsewhere.<sup>15</sup>

**Investigations under Oxidizing Atmosphere.** Thermogravimetric examinations reflect the mass effects during the removal of water and template from the pores of the crystals under continuous heating at a constant rate. The measurements, according to method 1 (Figure 2, Table 1), show the characteristic shape with two main mass loss regions: the low-temperature region between 423 and 623 K with the maximum at  $513 \pm 5$  K (peak P1) and the high-temperature region between 623 and 1123 K with the maximum between 748 and 843 K

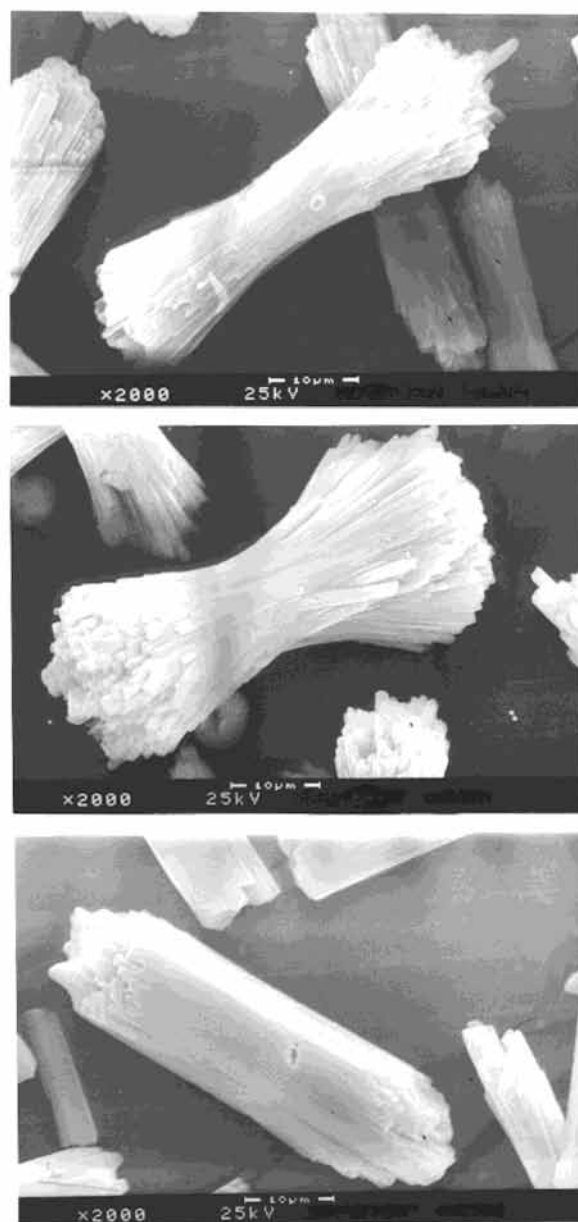


**Figure 1.** SEM micrographs of (A, top)  $\text{AlPO}_4\text{-31}$  and (B, middle)  $\text{CrAPO-31}$  (sample 4) as examples of the morphological characteristic of all the metal-substituted derivatives except (C, bottom)  $\text{ZnAPO-31}$ , which has a different morphology (sample 15).

(peak P2). All samples, together with nondoped  $\text{AlPO}_4\text{-31}$ , also show mass loss at a temperature below 423 K, which is attributed to a partial release of water. The latter relatively small loss suggests that (i) the samples, which were dried at 378 K overnight and next rehydrated by contact with open atmosphere for several days, do not reveal a considerable readsorption of water and (ii) the released water comes predominantly from the external surface, while another part is more strongly restrained from leaving the crystals and requires conditions which correspond to the low-temperature region.

The low-temperature peak shows an asymmetric shape (with the exception of  $\text{AlPO}_4\text{-31}$ ) and a tendency to split into two constituent peaks with increasing heteroatom content (Figure 2). This indicates that two processes are running in parallel or in very close sequence: (i) release of occluded water and (ii) release of the products of template decomposition or template itself. A more precise determination of the positions and/or

TABLE 1: Characteristics of the Examined MeAPO-31 Materials

no.	Me	Me/(Al <sub>2</sub> O <sub>3</sub> + P <sub>2</sub> O <sub>5</sub> ) in		Me/uc	uc/Me	P1 <sup>a</sup> (K)	P2 <sup>b</sup> (K)	F <sup>c</sup>	$\Delta m^d$ (%)		
		reaction gel	calcined sample						under O <sub>2</sub>	under O <sub>2</sub> (ground)	under N <sub>2</sub>
1	AlPO					508	748	0.75	8.85	11.38	11.22
2	Cu	0.0050	0.00075	0.0135	74.1	513	788	0.95	9.07	10.19	10.12
3	Cd	0.0050	0.00090	0.0162	61.7	508	783	0.97	8.96	9.81	9.90
4	Cr	0.0025	0.00048	0.0087	114.5	513	793	0.95	9.16	10.53	10.10
5	Cr	0.0050	0.00089	0.0161	62.1	513	803	1.29	8.97	11.79	10.29
6	Co	0.0025	0.0019	0.0345	29.1	508	793	1.20	9.06	11.40	11.06
7	Co	0.0050	0.0036	0.0648	15.4	508	808	1.56	8.92	10.35	10.21
8	Co	0.0050	0.0038	0.0675	14.8	523	813	1.69	8.94	10.72	9.89
9	Mn	0.0025	0.0025	0.0453	22.0	518	798	1.26	8.99	10.18	10.09
10	Mn	0.0050	0.0047	0.0846	11.8	513	813	1.88	9.08	10.13	9.73
11	Mn	0.0050	0.0049	0.0873	11.6	518	813	1.60	9.07	10.55	9.88
12	Mg	0.0025	0.0039	0.0703	14.2	513	803	1.27	9.14	10.97	10.68
13	Mg	0.0050	0.0073	0.1323	7.6	513	823	1.77	9.10	10.44	9.69
14	Mg	0.0050	0.0076	0.1368	7.3	518	833	1.86	8.90	10.73	9.97
15	Zn	0.0025	0.0043	0.0770	13.0	518	803	1.55	9.10	10.07	9.52
16	Zn	0.0025	0.0057	0.1030	9.8	513	823	1.80	9.13	9.65	9.31
17	Zn	0.0050	0.0100	0.1910	5.2	518	838	2.21	9.15	10.22	8.47
18	Zn	0.0050	0.0120	0.2140	4.7	518	843	2.31	9.13	9.94	9.87

<sup>a</sup> P1 is the maximum of the low-temperature peak. <sup>b</sup> P2 is the maximum of the high-temperature peak; <sup>c</sup> F is the intensity ratio of high-temperature peak P2 to low-temperature peak P1. <sup>d</sup>  $\Delta m$  is the total mass loss of the sample between 303 and 1273 K.

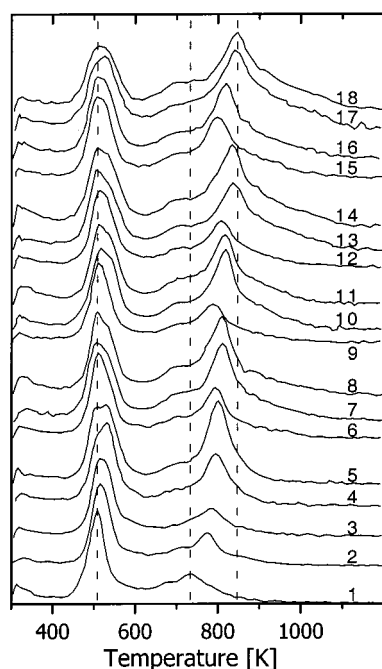


Figure 2. DTG curves of MeAPO-31 materials recorded under oxygen atmosphere (numbers refer to samples shown in Table 1).

relative intensities of both constituent peaks is not possible due to a significant overlap. However, it seems very likely that part of the template has first to leave the channels or to be burned, to open the way for the water molecules trapped deeper inside the pores. The position of the single P1 peak for nonsubstituted AlPO<sub>4</sub>-31 located at the lower temperature constituent peak also strongly suggests such a mechanism, i.e., that this lower temperature constituent peak corresponds to template and the higher one to water removal.

As opposed to peak P1, the high-temperature DTG peak P2 (Figure 2, Table 1) should be attributed fully to the burning of the template. While the low-temperature peak (P1) always occurs at a constant temperature, the high-temperature peak (P2) shifts from 748 K (AlPO<sub>4</sub>-31) to 843 K (ZnAPO-31), following the increasing content of heteroatoms (Table 1, Figures 2 and 3). Simultaneously, the relative intensity ratio of the high-

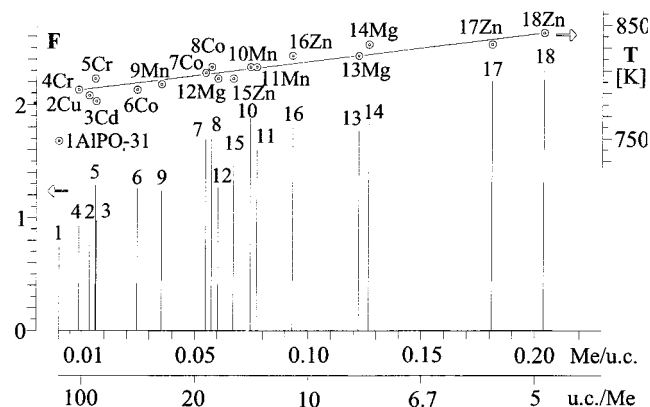


Figure 3. Temperature positions of the high-temperature peaks (right axis) and intensity ratios  $F = P2/P1$  between the high- and low-temperature DTG peaks (left axis) as functions of the metal content in MeAPO-31 materials.

low-temperature peaks,  $F = P2/P1$ , which reflects the ratio of the mass losses within both temperature regions, increases systematically with the content of heteroatoms from ca. 0.7 for AlPO<sub>4</sub>-31 (sample 1) to 2.3 for ZnAPO-31 (sample 18) (Table 1, Figure 3). However, the total intensity of both peaks is constant and corresponds to  $7.2 \pm 0.2\%$  mass loss under calcination above 423 K. Thus, the mass loss at the lower temperature (P1) diminishes continuously, which indicates that the removal of template becomes more difficult when the content of substituted metals is increasing. This can result from increased interactions between the template molecules located in the pores and the more numerous metal heteroatoms of the framework.<sup>4</sup> These facts support the conclusions above (cf. the previous paragraph), which stated that the low-temperature peak P1 corresponds partially to water and partially to template removal. Moreover, this suggestion is supported by the fact that the lower-temperature constituent peak of P1 belongs to the template, as this constituent decreases more intensively with the content of metals than the other one. This consequently means that a significant portion of water is unable to leave the channels before the template is removed. This is also in agreement with the ATO-type structure. Its 6-rings are too small to enable water to leave the crystals "throughout the walls" as in the case of AlPO<sub>4</sub>-5.<sup>4</sup>

The constant position of the low-temperature peaks P1 indicates that the energy necessary for the corresponding processes is independent of the sample composition. Thus, these peaks seem to reflect the removal of molecules which, apparently, are simply occluded in the pores and can freely leave them. Such interpretation has already been proposed by us<sup>14</sup> for the MeAPSO-11 materials, and for various aluminophosphates by other authors.<sup>8,9,13</sup> The temperature of the peak P1 corresponds to the transformation of the structure (XRD) from triclinic to rhombohedral<sup>15</sup> and indicates a direct correlation between the structure symmetry and the content of molecules in the pores.

The changes described for the high-temperature peak P2 indicate significant mutual interactions between the sorption centers of the metal heteroatoms in the framework and template molecules. Otherwise, the high-temperature peak would only represent the oxidative destruction of the amine, which should occur at a constant temperature. The temperature at which the products of template decomposition finally leave the pores (P2 peak maximum) increases in proportion to the content of metals in the crystals (Figure 3): within experimental error, one can draw a straight line through the points corresponding to particular samples and nondoped AlPO<sub>4</sub>-31 (Figure 3). This straight line confirms the existence of a direct dependence. Such a tendency is also well pronounced for the intensity ratio of the peaks,  $F = P2/P1$  (Figure 3): the amount of the template molecules which cannot leave the pores within the low-temperature region P1 increases in proportion to the content of heteroatoms. Due to the observed scattering of the experimental points in the plot, it is difficult to decide if the samples with various heteroatoms may exhibit separate dependences. Nevertheless, they seem to be close to each other. In other words, an increase in the amount of framework heterocenters is accompanied by an increase in the number of template molecules that are obstructed in leaving the pores, in an unaffected form or decomposed, within the low-temperature region. Consequently, it can be concluded that the high-temperature region reflects not only a simple oxidative destruction of the template,<sup>13</sup> but also a complex process of template destruction/oxidation, followed by a temperature-forced removal/desorption of these destruction products. If these products are really increasingly hindered from removal with increasing content of heteroatoms, the observed shift of the P2 temperature can be well justified. However, this could also be an artificial effect originating from the time delay of desorption at a constant heating rate of the samples. This has been decided on the basis of the other results (see below).

In general, the discussed DTG effects might formally imply that the template molecules retained by the studied crystals of ATO structure type (as well as those of AEL<sup>14</sup> and AFI<sup>17</sup> types) can be divided into two groups:

(i) template molecules which are (especially in the case of the lack of sorption centers, i.e., heteroatoms, in the framework) easy to remove from the pores in any form under relatively mild heat treatment;

(ii) template molecules bonded to, or interacting with, the heteroatoms or other sorption centers of the framework, which are less mobile and require more severe heat treatment and/or an oxidative destruction for the removal. A higher content of such molecules may cause a lower packing density<sup>14</sup> of template in the pores.

The insight into the desorption mechanisms came from the measurements with method 2 and the mass spectra. The latter (not shown) indicated a predominant removal of CO<sub>2</sub> and H<sub>2</sub>O,

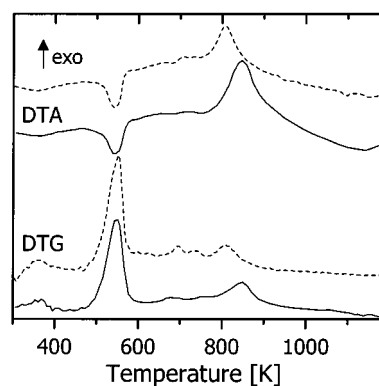


**Figure 4.** DTG and DTA curves for ZnAPO-31 (16) (full lines) and MnAPO-31 (9) (dotted lines) recorded in air atmosphere.

especially in the regions of both DTG peaks. Several fragments of higher mass up to  $M = 96$  were also recorded, but in amounts lower by 2–3 orders of magnitude than the main products. Interestingly, no traces of N<sub>2</sub>, NO, NO<sub>2</sub>, NH<sub>3</sub>, or CO were observed. Thus, the mass spectra proved that the low-temperature DTG region reflects a decomposition or destruction and not a simple desorption of the template since its mass of 101 was not detected. However, the DTA curves (Figure 4) showed that the process is endothermic and not exothermic as would be expected as the result of oxidation. Evidently, the exothermic oxidation is overcompensated by endothermic effects of template destruction (e.g., cracking) and desorption of water. This consequently confirms the above conclusions that larger amounts of water are trapped by the template molecules in the channels and cannot exit before the template leaves the pores. It should then be accepted that the low-temperature peak P1 corresponds predominantly to the desorption of water while the oxidation and destruction of template account for only a smaller contribution. Interestingly, the weight losses under an oxidizing atmosphere from the unidimensional pore systems of MgAPO-50 (pore diameter 0.7–0.8 nm)<sup>9</sup> and MgAPO-39 (0.4 nm)<sup>8</sup> up to 710 and 579 K, respectively, have been interpreted as desorption of water and unaffected di-*n*-propylamine, while only the peaks at higher temperatures have been attributed to oxidative cracking of the template. This interpretation concerning the template cannot be verified on the basis of our results.

The above findings are in agreement with our IR and Raman studies on the removal of triethylamine template from the pores of AlPO<sub>4</sub>-5 materials.<sup>17</sup> These results have demonstrated that, within the temperature range below the high-temperature peak, a gradual decomposition of template occurs and that the process (i) is accompanied by simultaneous release of water and (ii) proceeds in a different way under oxygen and nitrogen atmospheres.

The high-temperature DTG region corresponds to a strongly exothermic DTA effect (Figure 4). This confirms that the large amounts of water and CO<sub>2</sub> observed in the mass spectra within this region originate predominantly from oxidation of the template and its destruction products. This is also in agreement with the spectroscopic findings for AlPO<sub>4</sub>-5,<sup>17</sup> which show that oxidation of the products from template destruction is the only process.

An additional support for the above conclusions is given by the DTG effects for nondoped AlPO<sub>4</sub>-31. As this material per se does not contain heteroatoms, its DTG profile should not exhibit any high-temperature peak. In fact, the ratio of the high- to low-temperature regions has the lowest value, which varies for different AlPO<sub>4</sub>-31 samples from 0.65 to 0.85. We interpret

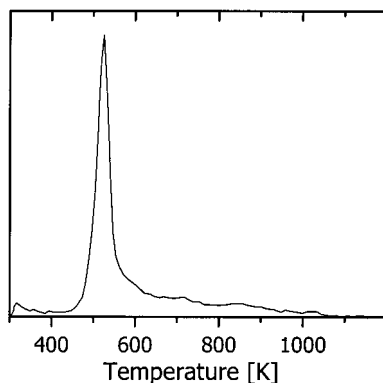


**Figure 5.** Thermogravimetric DTG profile of the undoped  $\text{AlPO}_4$ -31 material.

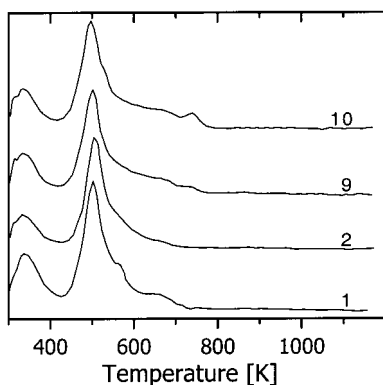


**Figure 6.** Selected examples of the DTG curves for ground MeAPO-31 materials recorded under oxygen atmosphere (for the sample numbers refer to Table 1).

this to be an effect of tiny amounts of heterocenters, i.e., structure defects or randomly incorporated heteroatoms originating from impurities in the reaction gels. Indeed, under modified conditions, we succeeded in synthesizing  $\text{AlPO}_4$ -31, which does not exhibit any high-temperature peak (Figure 5). This confirms that removal of the products of the template decomposition and oxidation as well as exiting of the water can proceed rapidly enough if they are not hindered by interactions with sorption centers. Noteworthy, the position of the single low-temperature peak corresponds to that of the similarly single DTG peak for the di-*n*-propylamine removal from the likewise unidimensional pores of  $\text{AlPO}_4$ -11.<sup>13</sup>

The total mass loss is constant for all samples studied and is equal to  $9.0 \pm 0.15\%$  (Table 1). Apparently, this observation is inconsistent with that of MeAPSO-11,<sup>14</sup> for which we have found a clear decrease in the total mass loss with an increasing content of heteroatoms. A similar effect has been reported for  $\text{CoAPO}$ -5.<sup>6</sup> Evidently, due to the low heteroatom content in the framework of the materials under investigation, the packing density of template in the pores is not markedly influenced by interactions between the heteroatoms and template.

The DTG measurements of the ground samples show practically only the first low-temperature peak (Figure 6). As grinding distinctly shortens the pathway for the products of template decomposition out of the pores and for oxygen into the pores, the lack of the high-temperature peak indicates that diffusivity is the factor determining the ability of the species considered to exit the pores. Therefore, the endothermic DTA effects (Figure 7), corresponding to the much stronger low-temperature DTG effects for the ground samples, become much weaker due to almost equilibrated processes of exothermic oxidation and

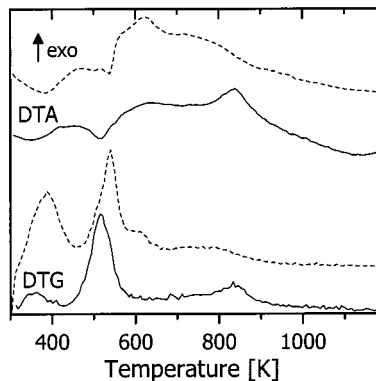


**Figure 7.** DTG and DTA curves for the ground samples of  $\text{ZnAPO}$ -31 (16) (full lines) and  $\text{MnAPO}$ -31 (9) (dotted lines) recorded in air atmosphere.

endothermic destruction of template and removal of water. In parallel, the main exothermic effect is shifted to a lower temperature (about 630 K) as a consequence of an improved access for oxygen.

The powdered samples reveal a larger total mass loss (Table 1) than the original crystals, which is related to a considerable increase in the water content (Figures 6 and 7, peak at ca. 350 K). Grinding resulted in an increase of surface and creation of numerous additional terminal OH groups which are new sorption centers for water. This is supported by a broader distribution ( $10.7 \pm 1.1\%$ , Table 1) of the values, which most likely reflects the differences in manual grinding of the samples.

Finally, the discussed shift of the high-temperature peak with the growing metal content (Figures 2 and 3) should be interpreted as the result of a composed phenomenon, including a number of distinct (thermo)chemical processes. This can also be concluded from the broadening of the peak, i.e., from the wide temperature range of the processes. With increasing metal content, more and more template molecules are prevented from leaving the channels within the low-temperature region. As this process is mainly dependent on the movability of the species in the pores and, on the other hand, the thermogravimetric measurements are based on a constant heating rate of the samples, the increasing number of template molecules which cannot be removed sufficiently fast causes the observed shift of the peak to a higher temperature.

**Investigations under an Inert Atmosphere.** The thermogravimetric measurements of the template removal under nitrogen and oxygen atmospheres give similar pictures of changes following the content of heteroatoms. The low-temperature peaks occur at the same position and are similarly split or asymmetric (Figure 8). This proves that the template removal occurring in this temperature region is controlled exclusively by energy and is independent of the chemical nature of the components.

The second effect of the mass loss occurs under nitrogen at a lower temperature and seems to be less than that under oxygen (Figures 8 and 9). All the processes are endothermic (Figure 9). The mass spectroscopy measurements indicate a clearly larger number of various mass fragments than that under an oxygen atmosphere. Relatively strong signals are observed for  $M = 17, 30, 31, 58, 72,$  and  $101$  which can be assigned to  $\text{NH}_3$ ,  $\text{CH}_3\text{NH}-$ ,  $\text{CH}_3\text{NH}_2$ ,  $\text{C}_3\text{H}_7\text{NH}-$ ,  $\text{C}_3\text{H}_7(\text{CH}_3)\text{N}-$ , and  $(\text{C}_3\text{H}_7)_2\text{NH}$  (not decomposed DPA). At lower contents of metals, the high-temperature peak P2 is observed at about 600 K as a shoulder of the P1 peak. Increasing amounts of metals in the molecular sieves caused a shift of the peak P2 up to about 690

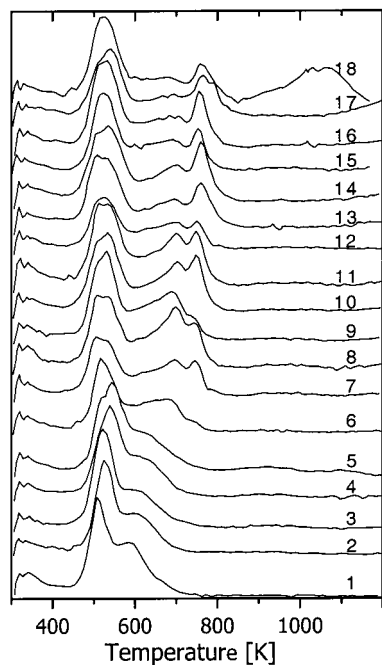


**Figure 8.** DTG curves of MeAPO-31 materials recorded under nitrogen atmosphere (for the sample numbers refer to Table 1).

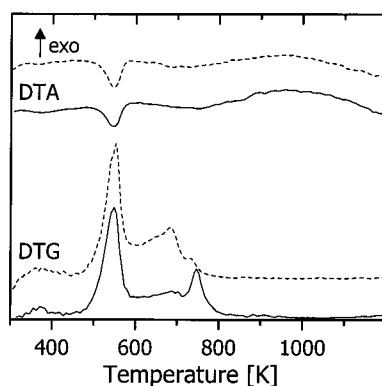


**Figure 9.** DTG and DTA curves for ZnAPO-31 (16) (full lines) and MnAPO-31 (9) (dotted lines) recorded in argon atmosphere.

K. This shift should be considered in a manner similar to that seen under oxygen, i.e., as transport-dependent and/or affected by the method. Nevertheless, the lower temperature of this peak indicates the occurrence of different chemical processes. Most likely, this temperature is high enough for a thermal decomposition of the template molecules into simpler products and easier release of them. It should mean, of course, that products formed at a temperature below 600 K under oxygen are thermally more stable than those formed under nitrogen. Surprisingly, the high-temperature peak recorded under nitrogen splits at higher metal contents into two constituent peaks, the second of which occurs at a constant position of about 780 K (Figure 8). The intensity of the latter constituent peak increases quickly with metal content while the other one decreases proportionally. This implies that, due to the coinciding kinetic and methodological (constant heating rate) reasons discussed above, a part of the template molecules undergo another reaction and, after that, can leave the pores only at a higher temperature.

The intensity ratio of the high-temperature (both components together) to low-temperature peaks increases with metal content in a manner similar to that under an oxygen atmosphere, though this effect is not as regular as for oxygen.

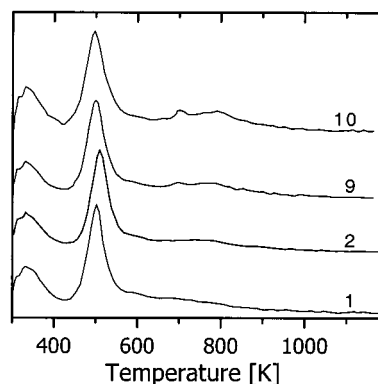


**Figure 10.** Selected examples of the DTG curves for ground MeAPO-31 materials recorded under nitrogen atmosphere (for the sample numbers refer to Table 1).

The total mass loss under a nitrogen atmosphere (Table 1) is higher than that under oxygen for all samples and is equal to ca.  $9.9 \pm 0.4\%$  with some exceptions. This was observed despite a gray color of the samples, indicating the occurrence of some quantities of unburned coke. Such observations were also reported for MgAPO-50<sup>9</sup> but not for MgAPO-39.<sup>8</sup> A similar effect for AlPO<sub>4</sub>-5 with tripropylamine has been related to the pretreatment of the sample.<sup>5</sup> For the MeAPO-31 materials in this study, the scattering of the values speaks more for secondary influences than for a feature of the system.

The behavior of the powdered samples under nitrogen atmosphere is very similar to that under oxygen. The DTG curves show a complete, or almost complete, disappearance of the high-temperature peak after the samples were ground (Figure 10). The DTA curves under argon reveal only endothermic effects which are more pronounced than those under oxygen. These observations support the above conclusions and the presumed diffusion-dependent mechanism of the template removal. An especially good confirmation is given by the enhanced desorption of di-*n*-propylamine and its fragments from the powdered sample in the low-temperature range. Amounts of these fragments measured by mass spectroscopy under Ar atmosphere are higher by 1 order of magnitude than those for the original crystals. Thus, the reactions at temperatures above the first low-temperature peak are the only stages of the removal that depend on the applied atmosphere. Most likely, an inert atmosphere generally favors a simple thermal decomposition of template. Under oxidizing conditions, more stable and higher molecular weight products containing oxygen are formed, which are less mobile and require a higher energy for removal. This conclusion corresponds well to the former findings by Choudhary and Sansare.<sup>5</sup>

The observed regular dependences also yielded a secondary result. The occurrence of a systematic dependence on very rare and statistically distributed extraframework metal species occluded in the pores should be logically excluded. Consequently, it can be concluded that our comparative DTG studies performed in a larger series appear to provide evidence, additional to the other methods, for the incorporation of the heteroatoms into the framework.

## Conclusions

All the investigated MeAPO-31 materials doped with very small amounts of Cu, Cd, Cr, Co, Mn, Mg, and Zn (1 Me atom per 5–115 unit cells) showed a direct dependence of the position of the high-temperature DTG peak and of the intensity ratio between the high- and the low-temperature DTG peaks on the

content of heteroatoms. Similarly to the XRD studies,<sup>15</sup> the thermoanalytic investigations showed that the primary factor controlling the properties of the materials is the content of the heterocenters and not their chemical identity. The measurements for the original and ground crystals under O<sub>2</sub> and N<sub>2</sub> atmospheres strongly imply that the removal of template from the pores by calcination is controlled by diffusion mechanisms, dependent on the content of metallic heterocenters and the dimensions of the crystals. It is expected that such a well-established dependence cannot be observed for higher contents of the metals in the studied molecular sieves, especially close to the limits when the framework becomes "saturated" with the metals. The template removal occurring in the range of the low-temperature DTG peak is controlled by energy only and is independent of the chemical nature of the heteroatoms. The chemical nature of the products of the template decomposition in the range of the high-temperature peak depends on the calcination atmosphere. With an increase in heteroatom content, the energy necessary to remove these products becomes higher.

The template molecules in the pores can apparently be divided into two groups:

(i) molecules capable of an easy decomposition and removal from the pores (it might be a part of the template located, e.g., in the surface region of the crystals);

(ii) molecules that cannot leave the pores quickly enough due to either a too long pathway or too many Me centers. These molecules are mostly bonded to or interact with the heterocenters of the framework and, therefore, can only be removed under a more severe heat treatment or/and oxidative destruction conditions. This condition seems to result partially from the time-dependent delay in release of template from the inside of the crystals. A higher content of this part of the template (especially possible at higher contents of heterocenters) may also result in a decreased packing density of the template molecules, which is already formed during the synthesis stage.

Water cannot leave the channels of as-prepared MeAPO-31 materials before removal of template due likely to steric hindrances and the too small dimensions of the 6-rings of the structure. This may explain the structure transformation<sup>15</sup> occurring at the temperature of water removal.

Comparative DTG investigations performed in series provide additional evidence for the isomorphous substitution of metals into the framework.

Further studies would be useful to confirm the inferred influence of heterocenters on diffusion in the pore system and thus on the calcination process. The best method for it seems to be a direct determination of *intracrystalline* diffusion with the NMR technique which has already been successfully applied for zeolitic adsorbents.<sup>18</sup>

**Acknowledgment.** This work was partially supported by the Deutsche Forschungsgemeinschaft (DFG) and by the Polish Committee for Scientific Research (KBN). Thanks are due to Dr. Jerzy Wloch (Nicholas Copernicus University) and Bernd Kersten (Berlin) for technical assistance.

## References and Notes

- (1) Wilson, S. T.; Lok, B. M.; Flanigen, E. M. US Patent 4,310,440, 1982.
- (2) Lok, B. M.; Messina, C. A.; Patton, R. L.; Gajek, R. T.; Cannan, T. R.; Flanigen, E. M. U.S. Patent 4,440,871, 1984.
- (3) Flanigen, E. M.; Lok, B. M.; Patton, R. L.; Wilson, S. T. *Proceedings of the 7<sup>th</sup> International Zeolite Conference*, Tokyo, 1986; Murakami, Y., Iijima, A., Ward, J. W., Eds.; Elsevier: Amsterdam, 1986; *Stud. Surf. Sci. Catal.* **1986**, 28, 103 and refs 9, 10, and 18–23 therein.
- (4) Kornatowski, J.; Zadrozna, G.; Wloch, J.; Rozwadowski, M. *Langmuir* **1999**, 15, 5863.
- (5) Choudhary, V. R.; Sansare, S. D. *J. Therm. Anal.* **1987**, 32, 777.
- (6) Shiralkar, V. P.; Saldarriaga, C. H.; Perez, J. O.; Clearfield, A.; Chen, M.; Anthony, R. G.; Donohue, J. A. *Zeolites* **1989**, 9, 474.
- (7) Minchev, Ch.; Minkov, V.; Penchev, V.; Weyda, H.; Lechert, H. *J. Therm. Anal.* **1991**, 37, 171.
- (8) Akolekar, D. B.; Kaliaguine, S. *Zeolites* **1994**, 14, 620.
- (9) Akolekar, D. B. *Zeolites* **1995**, 15, 583.
- (10) Tusar, N. N.; Kaucic, V.; Geremia, S.; Vlasis, G. *Zeolites* **1995**, 15, 708.
- (11) Rajic, N.; Gabrovsek, R.; Ristic, A.; Kaucic, V. *Thermochim. Acta* **1997**, 306, 31.
- (12) Rajic, N.; Gabrovsek, R.; Kaucic, V. *Thermochim. Acta* **2000**, 351, 119.
- (13) Ojo, A. F.; McCusker, L. B. *Zeolites* **1991**, 11, 460.
- (14) Kornatowski, J.; Finger, G.; Jancke, K.; Richter-Mendau, J.; Schultze, D.; Joswig, W.; Baur, W. H. *J. Chem. Soc., Faraday Trans.* **1994**, 90, 2141.
- (15) Finger, G.; Kornatowski, J.; Jancke, K.; Matschat, R.; Baur, W. H. *Microporous Mesoporous Mater.* **1999**, 33, 127.
- (16) Meier, W. M.; Olson, D. H.; Baerlocher, Ch. *Atlas of Zeolite Structure Types*; Elsevier: Amsterdam, 1992; *Zeolites* **1992**, 12.
- (17) Schnabel, K.-H.; Finger, G.; Kornatowski, J.; Löffler, E.; Peuker, Ch.; Pilz, W. *Microporous Mater.* **1997**, 11, 293.
- (18) Kukla, V.; Kornatowski, J.; Demuth, D.; Girnus, I.; Pfeifer, H.; Rees, L. V. C.; Schunk, S.; Unger, K. K.; Kärger, J. *Science* **1996**, 272, 702.